applied sciences

MDPI

Article

Design of Conical Foundations with Increased Bearing Capacity in Areas of Undermined Soils

Askar Zhussupbekov [1], Assel Sarsembayeva [1,*], Baurzhan Bazarov [2] and Abdulla Omarov [1]

[1] Department of Civil Engineering, L.N. Gumilyov Eurasian National University, Astana 010008, Kazakhstan; astana-geostroi@mail.ru (A.Z.); omarov_01@bk.ru (A.O.)
[2] Department of Civil Engineering, Karaganda Industrial University, Temirtau 101400, Kazakhstan; baur.bazarov@mail.ru
* Correspondence: assel_enu@mail.ru; Tel.: +7-7078503035

Abstract: This article discusses the foundations of a conical shape directed with their apex downwards to increase the cross-sectional area and, accordingly, the bearing capacity during settlement and under the influence of horizontal tensile strains in undermined areas. To simulate the deformability of undermined and seismically exposed foundations, a three-dimensional expandable box was manufactured and assembled. Models of a conical foundation with an aperture angle of the cones at 90° and 80° were buried into the soil at 0.75 of its height, in order to provide a safety margin for further loading due to an increase in the bearing area when the cone is immersed deeper into the ground. Laboratory and field tests were performed on the vertical loading of single cones before and after horizontal soil displacement. Numerical modeling of the interaction between soil and foundation was carried out for conical foundation models that were considered for laboratory and field testing using the Plaxis 2D (Version 8.2) program. To compare the bearing capacity, isolated shallow foundations with a diameter equal to the cross section of the conical foundation at the intersection with the ground surface were tested. The isolated shallow foundations lost their bearing capacity after 0.15 kN in laboratory tests and after 75 kN in the field tests, while the ultimate bearing capacity of conical foundations with the similar cross section at the soil surface was not achieved, even after 0.2 kN during laboratory tests with horizontal soil displacement and at a load of 100 kN in field tests.

Keywords: conical foundations; horizontal displacement of soils; load–settlement interaction; stable foundations; undermined soils

Citation: Zhussupbekov, A.; Sarsembayeva, A.; Bazarov, B.; Omarov, A. Design of Conical Foundations with Increased Bearing Capacity in Areas of Undermined Soils. *Appl. Sci.* **2024**, *14*, 1816. https://doi.org/10.3390/app14051816

Academic Editor: Eduardo Ferreira da Silva

Received: 8 December 2023
Revised: 19 February 2024
Accepted: 20 February 2024
Published: 22 February 2024

1. Introduction

A significant number of mines in the world (Australia, Canada, USA, South Africa, Russia and the countries of Central Asia, etc.) extract minerals in massifs exposed to high sub-horizontal tectonic stresses [1–5]. The violation of the natural stress–strain state of a rock mass during mining leads to rock fails and man-made earthquakes, destroying nearby buildings and threatening people's lives [6,7].

Systematic instrumental observations of the movement of the Earth's surface began to be carried out in 1928 on the initiative of Professor I.M. Bakhurin and made it possible to generalize the results of observations and identify dependencies for determining individual parameters of the displacement of the undermined surface [2]. These studies were continued by [8–10], who, having analyzed a large volume of observations of deformations and displacements of the Earth's surface, came to the conclusion that deformations of the Earth's surface can be represented as the result of bending and folding of surface layers of rocks and loose soils.

According to previous studies [2,10], it has been established that, based on the nature of rock formation in the undermined strata, three zones of displacement in height can be distinguished:

1. The collapse zone, where part of the undermined strata turns into an incoherent mass of loosened collapsed rocks.
2. Above it is a zone of cracks in which the structure and layering of the rocks is preserved, but their continuity is disrupted.
3. Above the zone of cracks is a zone of deflections without discontinuities, where the structure, layering and continuity of the rocks is preserved.

If the size of the mined-out space is large enough the displacement process reaches the Earth's surface, on which a depression is formed called a displacement trough, the area of which is always greater than the area of the excavation [9,11,12].

The shape and dimensions of the displacement trough depend on the depth and size of the excavation, the physical and mechanical properties of the undermined and overlying layers, etc. If complete displacements of the Earth's surface are achieved, the displacement trough takes the shape of a plate with a flat bottom. No further displacement occurs as the complete deformation takes place. With incomplete vertical displacement, the displacement trough of the Earth's surface takes on the shape of a bowl and entails a further increase in the area of the displacement trough [13].

According to the degree of influence on structures and the Earth's surface, two zones are distinguished: a zone of dangerous displacements exceeding the allowable deformations (limit values), and a zone of relatively safe displacements. The boundary of the displacement trough is located outside the zone of hazardous displacements and the possibility of placing structures on them depends on the subsidence of the Earth's surface, slope, curvature of convexity, concavity, horizontal displacements, existing ledges, and their height [9].

As a mineral layer is excavated, surface points alternately undergo three stages of deformation (Figure 1) [9,13]:

Stage I, the AB section, is characterized by positive curvature (convexity) and horizontal deformations.

Stage II, the BC section, is characterized by vertical curvature and horizontal compressive deformation.

Stage III is characterized as when all of the surface points fall into the flat bottom of the displacement trough with possible horizontal tensile deformations carried over from Stages 1 and 2.

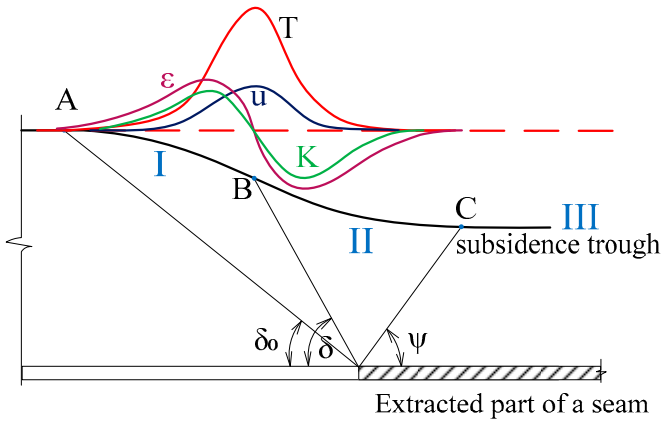

Figure 1. The subsidence trough and the distribution of surface deformation: δ_0, δ and ψ—the angles designating the boundaries of the zone of influence of underground mining along the strike of the formation; T—tilt; K—curvature; ε—horizontal strain; u—horizontal displacement.

The initial total stress of a soil element in a layer located at depth z from the Earth's surface is characterized by vertical stress σ_z:

$$\sigma_z = \gamma \cdot z \quad (1)$$

and horizontal stresses σ_x, σ_y by the axes x and y:

$$\sigma_x = \sigma_y = K_0 \cdot \gamma \cdot z \quad (2)$$

where K_0 = 0.6–1—lateral pressure coefficient.

The analysis of the mechanical properties of the undermined soil layer is influenced by cohesion c, modulus of elasticity during soil unloading E_{un}, tensile strength T, and angle of internal friction φ [5,9]. The horizontal tensile deformations are considered to be accompanied with curvature deformations of the convexity when tilted at Stage I [14]. Initially, tensile strains will reduce the magnitude of horizontal compressive stresses. Horizontal deformations σ_x change by the modulus of elasticity during soil unloading E_{un}:

$$\sigma_x = K_0 \gamma z \ - K_0 E_{un} \quad (3)$$

When the tensile strain exceeds the tensile strength of the soil, a crack is formed. The maximum possible depth of development of a rupture crack is limited by the fact that the blocks contoured by these cracks find themselves under conditions of uniaxial compression by gravity. Therefore, the maximum depth of cracks z_{max} is determined from the condition of equality of vertical stress σ_z to uniaxial compression:

$$\gamma z_{max} = 2c \cdot ctg\ (45^\circ - \varphi/2)$$

$$z_{max} = 2c/\gamma \cdot \text{ctg}\ (45^\circ - \varphi/2) \quad (4)$$

where c—cohesion, γ—bulk unit weight, φ—angle of internal friction.

A further increase in horizontal tension will be accompanied by the expansion of cracks, and below by plastic shear deformations without the formation of cracks (Figure 2).

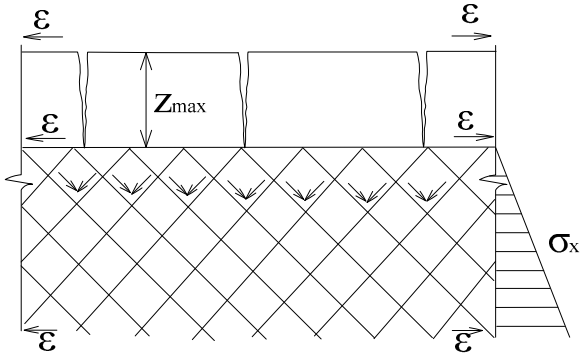

Figure 2. Deformations of the sediment layer at the contact with bedrock in the extension zone.

The stability of foundations in areas with increased horizontal tensile strains, namely in undermined areas, is important for the preservation of buildings and structures, as well as for reducing the destruction and cracks in buildings [14,15]. According to the Standard in Kazakhstan "SP RK 2.03-101-2012 Buildings and structures in mined areas and subsidence soils" [16] the displacement trough values, depending on the relative horizontal deformations and inclination, are divided into the following four groups of territories (Table 1):

Permission for the construction of buildings and structures in these territories is given on the basis of calculations of allowable deformations, including horizontal tensile deformations, which are measured as relative deformation in mm per meter of distance [17]. During the design, construction and operation process, soil displacement deformations are monitored. Observation geodetic stations, located in the form of profile lines along the strike and across the strike of the layers, record small movements of the soil in the horizontal plane. Observations in the vertical plane are determined by leveling, and in the horizontal plane by measuring the intervals between benchmarks.

Table 1. Groups of territories in undermined areas.

Groups of Territories	Relative Horizontal Deformation ε, mm/m	Inclination I, mm/m	Radius of Curvature R, km
1	$12 \geq \varepsilon > 8$	$20 \geq \varepsilon > 10$	$1 \leq R < 3$
2	$8 \geq \varepsilon > 5$	$10 \geq \varepsilon > 7$	$3 \leq R < 7$
3	$5 \geq \varepsilon > 3$	$7 \geq \varepsilon > 5$	$7 \leq R < 12$
4	$3 \geq \varepsilon > 0$	$5 \geq \varepsilon > 0$	$12 \leq R < 20$

Considering the operational features of existing traditional forms of foundations (strip, free-standing, prismatic pyramidal), it turned out that under the influence of horizontal displacements in mine workings, there is not a sufficient contact area between the foundation structure and the soil to ensure the stability of the foundation, especially with horizontal tensile deformations [15,18]. So, the study of the influence of horizontal deformations of the undermined base along the base of strip foundations was carried out by V.P. Kozlov [11], and for pile foundations [19] and the stability of dam on undermined soils by Zhussupbekov et al. [20]. Full-scale studies of the force effects of horizontal deformations on the lateral surfaces of the foundations of undermined buildings were carried out by Kozlov and Avershin [10,11]. A case study of building damage risk assessment due to deep excavation was analyzed by Lee et al. [21].

The conical model, which was commonly used for offshore structures, was considered as a basis for the new sustainable models in recent years. Li et al. proposed a one-piece cone-shaped hollow flexible reinforced concrete foundation (CHFRF) for a mountain wind turbine [22,23]. A rubber layer was placed beneath the CHFRF to increase the foundation flexibility to resist cyclic and dynamic loadings and to increase the bearing capacity. Nguyen Van et al. used machine learning regression approach for the analysis of bearing capacity of conical foundations in clayey soils to understand the sensitivity of bearing capacity, including failure mechanisms, cone apex angle, embedded depth to height ratio, strength gradient ratio, anisotropic ratio and cone shape [24]. According to Nguyen Van et al. modeling the bearing capacity factor F was strongly affected by cone apex angle 100%, while strength gradient ratio, embedded depth ratio, and anisotropic ratio were a lower ranking of influence within the relative importance index at 91.52%, 90.73%, and 17.19%, respectively. The highest bearing capacity of a conical foundation was determined at 0 immersion level of the cone, that is, when the base of the cone does not sink below ground surface level, while the angle at the apex of the cone of 30–60° had a greater load-bearing capacity [24]. Although Chouhan et al. [25] were studying the dependence of vertical bearing capacity factors for the conical footing on base roughness, the angle of internal friction of soil and different apex angles, by performing two-dimensional lower and upper bound finite element limit analysis (FELA), determined that load bearing capacity increased with an increase in the apex angle of the conical footing from 30° to 180°. Theoretical analysis has been also carried out by Houlsby and Martin [26], Chakraborty and Kumar [27]. Cassidy and Houlsby, using the numerical method of characteristics in the FIELD program, calculated the destructive loads to determine the bearing capacity using an axisymmetric problem and derived the general shear failure mechanism of the conical model [28].

Since the previous authors limited themselves to only theoretical analysis and modeling, it was decided to test the conical foundation model in the laboratory and at the test site for the purpose of further research for use in civil engineering as the foundations of buildings and structures. A test method has been developed that simulates horizontal displacement of the soil in the laboratory conditions. Full-scale tests were limited by the ability to regulate soil movements and deformations and were carried out on real observations. The main goal of the research was to study effectively responsive stable foundations of a conical shape that are resistant to horizontal tensile deformations of soil masses in undermined areas, in order to prevent emergency situations and, as a result, reduce construction costs. Based on the results of computer modeling by previous authors,

as well as preliminary laboratory tests with samples, conical models with opening angles of 90° and 80° were selected as the model of the conical foundation under study.

2. Materials and Methods

The "load–settlement" interaction under the influence of horizontal forces on the soil stratum has an elastic character at the first stage and does not differ from a column foundation with an identical cross-sectional area at the level of its contact with the soil. However, the achievement of the limiting state for a conical foundation is much later than for an isolated shallow one. This phenomenon is explained by an increase in the cross-sectional area as it deepens into the base soil with horizontal movements, which accordingly increases the bearing capacity of the undermined base. Reducing the impact of horizontal forces on the structure of the upper part of the building is achieved by a rolling joint (Figure 3). However, the presence of a rolling joint practically does not eliminate the effect of horizontal forces on the underground part of the building. The use of a combination of a roller bed between the upper plane of the conical base foundation and the lower plane of the rigid basement plinth of the building determines a fundamentally new mechanism for the operation of conical foundations in undermined areas.

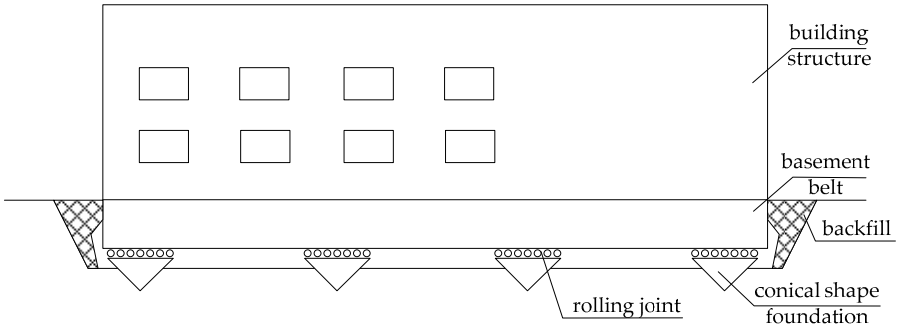

Figure 3. Design of a building on conical foundations with deformation joint.

The design of the conical foundation was proposed as partially immersed into the soil base with its apex downwards. Such positioning of the structure increases its load-bearing capacity under the influence of undermining impacts, since the area of the cone foundation structure increases with its immersion into the soils; that is, the settlement of the conical foundation has a positive effect on the bearing capacity of said conical foundation. The round shape of the base of the inverted cone avoids stress concentration near the corners and the formation of cracks at corner points.

In this work, models of foundation blocks of a right circular cone shape were used. A cone with aperture α was immersed in the ground to a depth of 0.75 height of the cone in order to provide a safety margin by increasing the diameter and, accordingly, the bearing area when loading the conical block (Figure 4). Based on previous studies [24,25], the opening angle of the cones α was taken as the average value from the previously considered modeling methods, and based on the results of preliminary laboratory tests, cones with an opening angle of 80–90° were considered in this study.

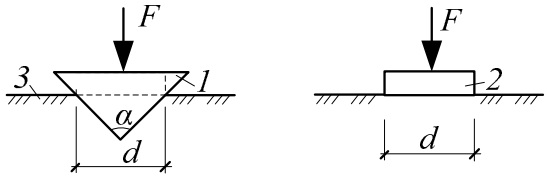

Figure 4. Loading of conical and isolated shallow foundations: d—diameter of conical foundations at the level of the soil base surface; 1—conical foundation; 2—isolated shallow foundation; 3—base soil; α—cone opening angle.

The cross-sectional area of the cone at an intersection with the soil's surface is determined by the formula:

$$A = F/R \quad (5)$$

where: A—cross-section area at the level of the ground surface; F—load applied to the surface of the foundation; R—ultimate bearing capacity of soil.

Comparative loading experiments of conical and isolated shallow foundation models with the same diameter were carried out to determine the settlement and the bearing capacity of soils under the horizontal soil displacement caused by horizontal tensile strains in undermined areas. When considering the behavior of the soil strata, special attention was paid to visual observation of the fracturing of the massif. The theoretical values of the maximum crack opening value were found by Formula (4).

2.1. Laboratory Testing

An expanding box, consisting of steel channels and a sealing of thick rubber is bolted together (Figure 5). Unscrewing the bolts leads to the expansion of the rubber spacer between the channel sections and, accordingly, extension of the box in length. This design of a sliding box allows you to simulate soil deformation caused by horizontal tension mentioned in Figure 2.

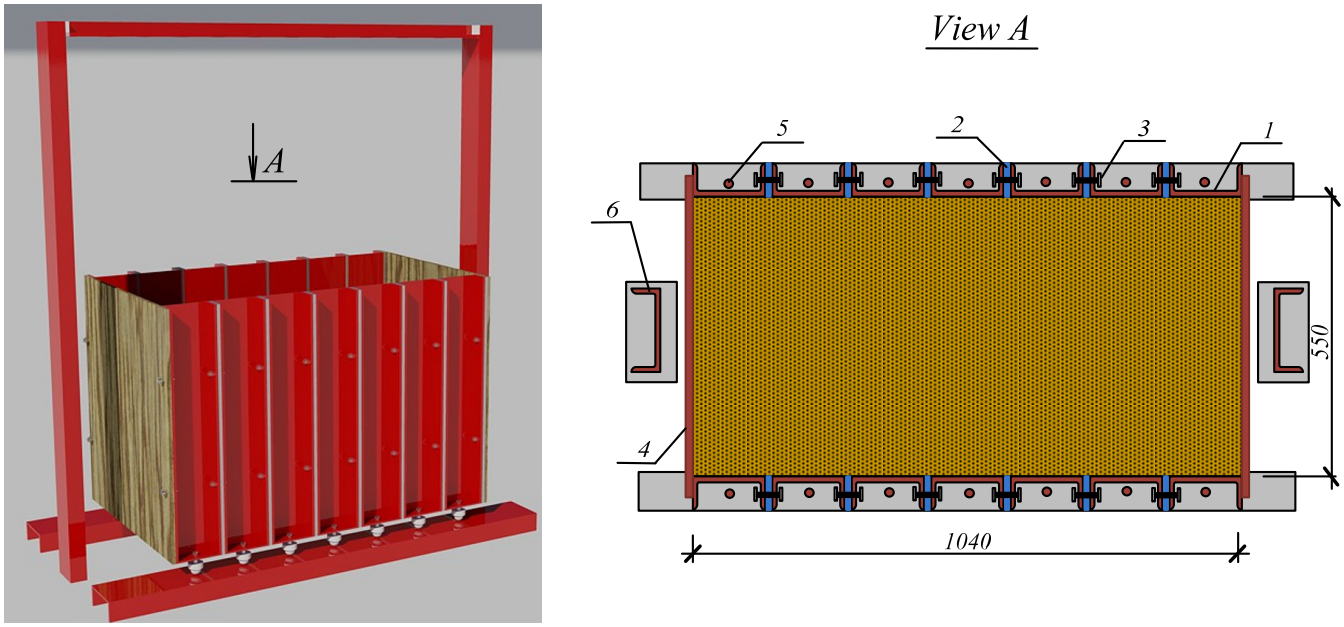

(**a**) (**b**)

Figure 5. Volumetric expandable box: (**a**) general view; (**b**) top view, 1—individual channel sections, 2—compressed elastic gaskets, 3—bolted connections, 4—side walls, 5—height-adjustable supports, 6—support frame.

Handmade soils were compacted by 5 cm layers with a 10 kg roller into the volumetric expandable box. During the compaction process, the density of the material was controlled by its specific weight. The soil used was an artificial soil selected using the equivalent materials method [18], which considers the processes of destruction and deformation of rock masses. The equivalent material was the replication of natural soils of the Karaganda region and made by mixing 97% fine sand and 3% spindle oil to increase viscosity and cohesion in the range of 0.5–1 kPa. The main physical and mechanical characteristics are presented in Table 2.

Table 2. Physical and mechanical characteristics of the testing soils.

Soil Characteristics	Units	Natural Soils	Equivalent Material
bulk unit weight, γ	kN/m^3	20.5	17
cohesion, c	kPa	40.0	0.9
angle of internal friction, φ	degree	29	37
modulus of deformation, E	MPa	-	0.24
Poisson ratio, ν	-	-	0.25

For given values of cohesion for natural soil and equivalent material, the modeling scale is:

$$m_l = l/L = C_m/C_n \cdot \gamma_m/\gamma_n \quad (6)$$

where $l/L = m_l$—linear scale;

γ_m, γ_n—specific gravity of model and natural materials;

C_m, C_n—cohesion of model material and soil in real conditions on the site (natural condition);

Thus, $m_l = 0.9/40 \times 20.5/17.0 = 1/40$.

The modeling scale in the experiments was taken to be 1/40. Models of conical foundations with a diameter of D = 80 mm and a height of H = 40 mm were made of aluminum alloy with an aperture (apex) angle of 90°, a diameter of D = 78 mm and a height of H = 46 mm with an aperture (apex) angle 80° and conical models with stand pile (Figure 6).

Figure 6. Cone foundation model.

The conical model foundation from aluminum alloy and concrete were placed on the compacted soil immersed 0.75 height into the ground. Laboratory tests of conical and isolated shallow foundation models are presented in Figure 7. The load on the foundation models was transferred statically in steps of 0.001 MPa and is maintained until the settlement is conditionally stabilized, which is taken to be a settlement of less than 0.01 mm in 15 min. The foundation model was loaded with surcharges weight until the specific pressure under the footing reached P = 16.7 kN/m^2. The settlement of the cone model foundations was measured with vertical dial gauges with reading accuracy up to 0.01 mm. The maximum load was taken to be the load from which the model lost its load-bearing capacity, and its settlement/movement became continuous. Horizontal tensile strains were achieved by unscrewing the joint between the channel sections and extending the box length by 3, 6, 9 mm/m. This caused horizontal soil movement and the displacement of the foundation models, which were monitored both vertically and horizontally.

(**a**) (**b**)

Figure 7. Laboratory testing of: (**a**) tests on the volumetric expandable stand; (**b**) loading of conical shape and isolated shallow foundation models.

Soil movement was monitored by measuring the distance between marks located on the ground surface 5 cm apart. Each experiment consisted of 5 loading stages: before horizontal ground displacements, at 3, 6, 9 mm horizontal soil displacements, and after stopping the horizontal displacement of the soil.

2.2. Field Test

Conical foundations with a 100 cm base diameter and 50 cm height for aperture angle 90°, and a 96 cm base diameter and 60 cm height for aperture angle 80° were manufactured and tested for static load at the experimental site (Figure 8).

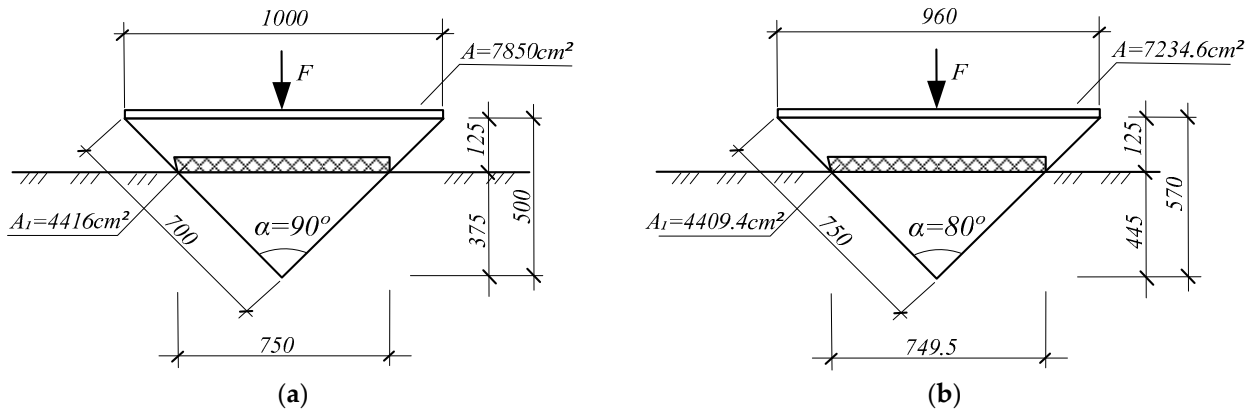

(**a**) (**b**)

Figure 8. Cone shape foundations: (**a**) with aperture angle 90°; (**b**) with aperture angle 80°.

The experiment area was located on the field of the Kostenko mine, Karaganda region (Kazakhstan). The soils on the site consisted of a topsoil layer, brown carbonate sandy loams with fine and medium sands (layer thickness 0.2–1 m) and dark gray, hard loams (layer thickness 2–6 m), which are detailed in Table 3.

Table 3. Physical–mechanical characteristics of the soils on the site.

Soil Characteristics	Units	Clayey Soils at Depth, m		
		2.5	4.5	6.0
bulk unit weight at natural moisture content, γ	kN/m^3	21.2	20.8	20.7
moisture content, w	%	11.8	12.1	29.0
liquid limit, WL	%	23	24	22
plastic limit, WP	%	21	18	19
cohesion, c	kPa	39	42	25
angle of internal friction, φ	degree	25	21	31
modulus of deformation, E	MPa	21.8	28.1	19.5

To observe the deformations of the Earth's surface caused by underground mining, measuring benchmarks were installed on a 3 × 3 m grid with a depth of 1.5 m. The location of the experimental foundation models was inside the grid. The load on the foundation under test was transferred using metal surcharges weighing 12.5 kN. The settlements of the foundations were determined by Aistov deflectometers placed through the axis passing over the center of the foundation being tested (Figure 9).

(**a**)

(**b**)

Figure 9. Field test: (**a**) cone shape foundations with aperture angle 90°; (**b**) isolated shallow foundation.

To compare the impact of isolated shallow foundations with conical ones, plate stamps with dimensions corresponding to the diameter at the intersection of the conical foundations with the ground surface were also tested for static loading. The area of the plates was $A_1 = 0.4416$ m^2. Metal balls with a diameter of 50 mm, fixed on a steel plate with dimensions of 500 × 500 × 20 mm using viscous oils were used as a rolling expansion joint. The number of balls was determined by the design load, so that the load on each ball did not exceed the contact strength of the material.

Since during the period of testing foundations for static loading only 2.6 mm of horizontal displacement of the soil mass was recorded on the site, this particular value of horizontal displacement was considered when comparing the bearing capacity before and after soil movement.

2.3. Numerical Study

The conical foundation was modeled using numerical calculation methods using the Plaxis 2D program. Due to the axisymmetric nature of the problem, a two-dimensional (2D) axisymmetric finite element (FE) formulation is used to model the soil domain and conical footing. The soil parameters obtained during laboratory tests were taken as the initial parameters. For the boundary dimensions of the site, the dimensions of the expanding stand were used. Load curves were obtained by modeling the loading of a conical up to 0.20 kN and isolated shallow foundation up to 0.15 kN. Loading for conical foundations modeling was set without soil displacement (Figure 10) and with horizontal displacement of 3, 6, 9 mm (Figure 11).

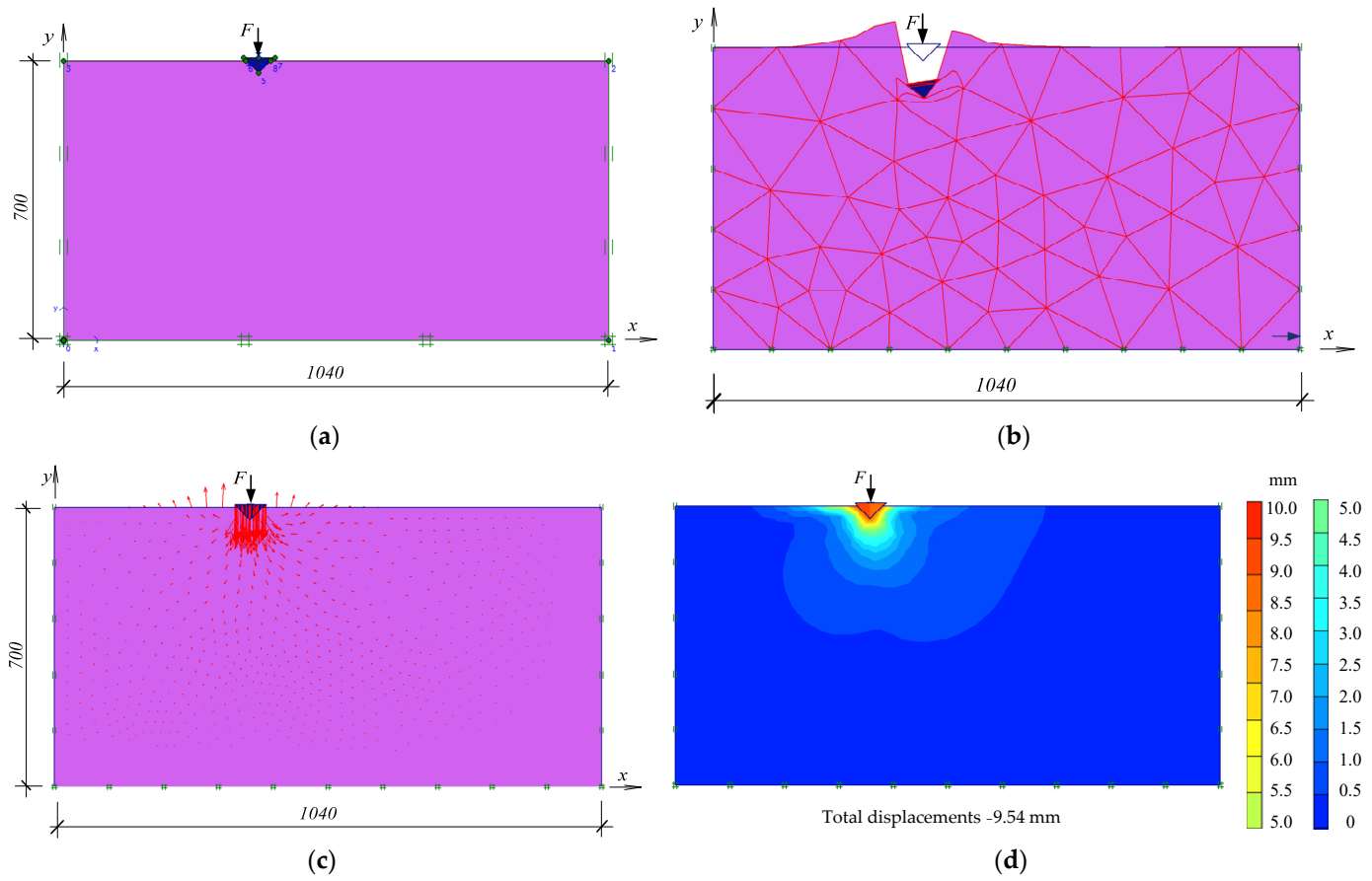

Figure 10. Numerical modeling of the conical foundation without horizontal displacement of the soil: (**a**) setting initial loading parameters; (**b**) deformed mesh; (**c**) displacement vectors; (**d**) total displacement.

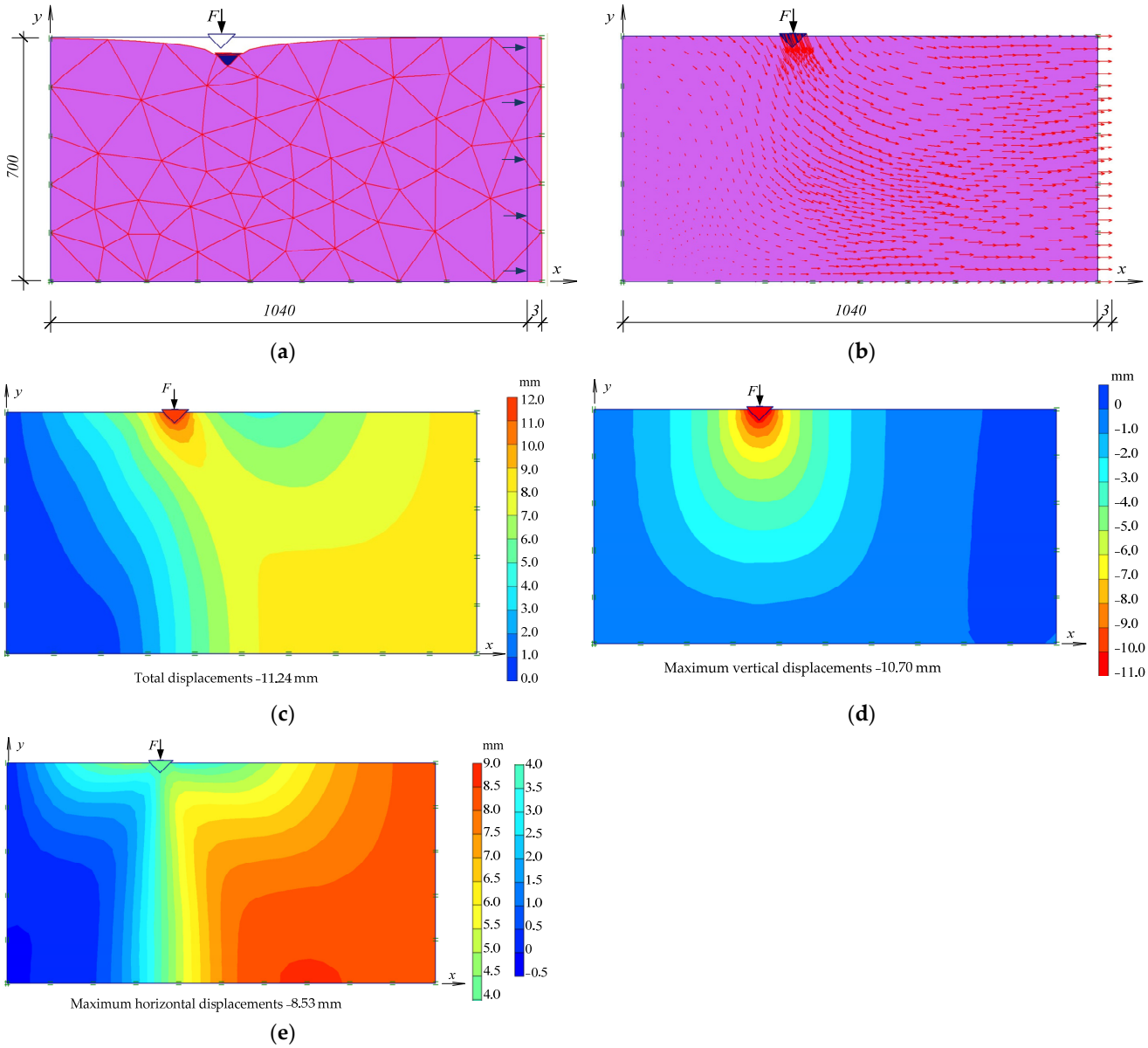

Figure 11. Numerical modeling results of a conical foundation with a horizontal soil displacement of 3 mm in the extendable stand: (**a**) deformed mesh; (**b**) displacement vectors; (**c**) total displacement; (**d**) vertical displacement; (**e**) horizontal displacement.

Deformed mesh was generated automatically with the Plaxis 2D program. The average element size and the number of generated triangular elements depend on the global coarseness setting. The global coarseness setting was set to medium, with 328 triangular elements. During the modeling, vertical and horizontal soil movements were considered, as well as total displacements. When modeling the bearing capacity of isolated shallow foundations, two loading cases were considered: without horizontal soil movement and with horizontal soil displacement ε = 3 mm (Figure 12). The initial data for modeling and soil properties were identical to those in laboratory tests.

The load was applied to the center of the foundation model, and the horizontal displacement of the soil was achieved by moving one end wall of the container with soil and extension of its size (Figure 5).

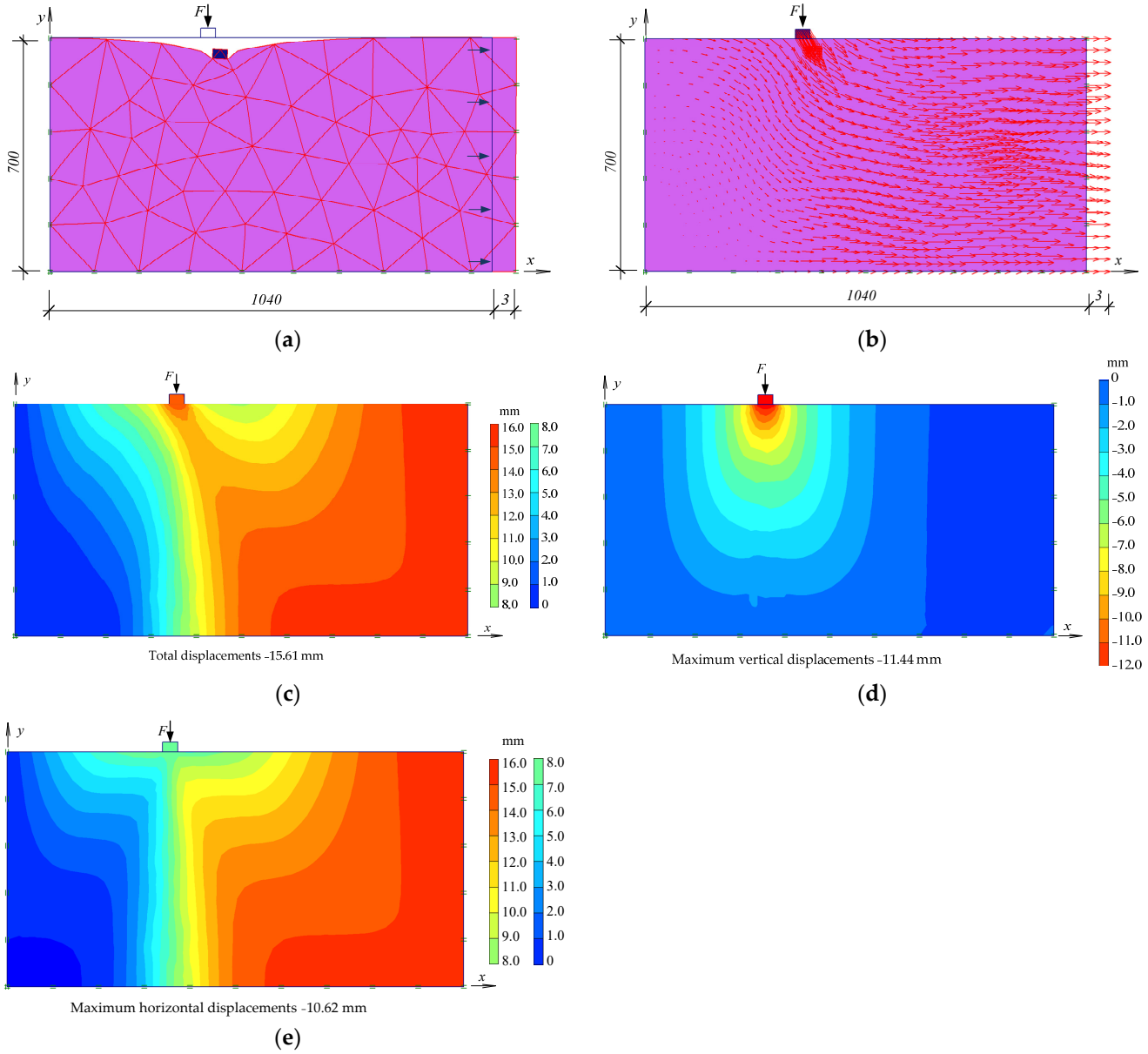

Figure 12. Numerical modeling results of an isolated shallow foundation under 0.15 kN load with a horizontal soil displacement of 3 mm in the extendable stand: (**a**) deformed mesh; (**b**) displacement vectors; (**c**) total displacement; (**d**) vertical displacement; (**e**) horizontal displacement.

3. Results

According to the data given in Table 4, the theoretical value determined by Formula (4) was that z_{max} was 18.3 mm, while observations during model tests in a volume-expandable stand at horizontal tensile deformation ε = 9 mm showed that the distance between cracks is about 9–10 mm and crack opening is about 0.5–1 mm. When transferred to real dimensions of soil displacement, these cracks are equivalent to a distance step of 2–4 m and an opening width of 32–44 mm. With a deformation of 3 mm, microcracks were detected in the equivalent soil at intervals of 10–20 mm, some of which increased to 0.8–1.5 mm with further expansion of the box. The frequency of crack opening was higher at the surface and decreased with depth.

A comparison of the settlement of conical and column foundations under load demonstrated a clear advantage in favor of the first type, since as the settlement raises to 6 mm, the bearing area increases by 1.22 times when the aperture angle of the conical model is 90° (Figure 13a). And after applying a load of 0.15 kN, the isolated shallow founda-

tion completely loses its load-bearing capacity. With horizontal soil displacement, the maximum load-bearing capacity of an isolated shallow foundation is limited to 0.15 kN, while for conical foundation models it is much higher due to an increase in the foundation support area.

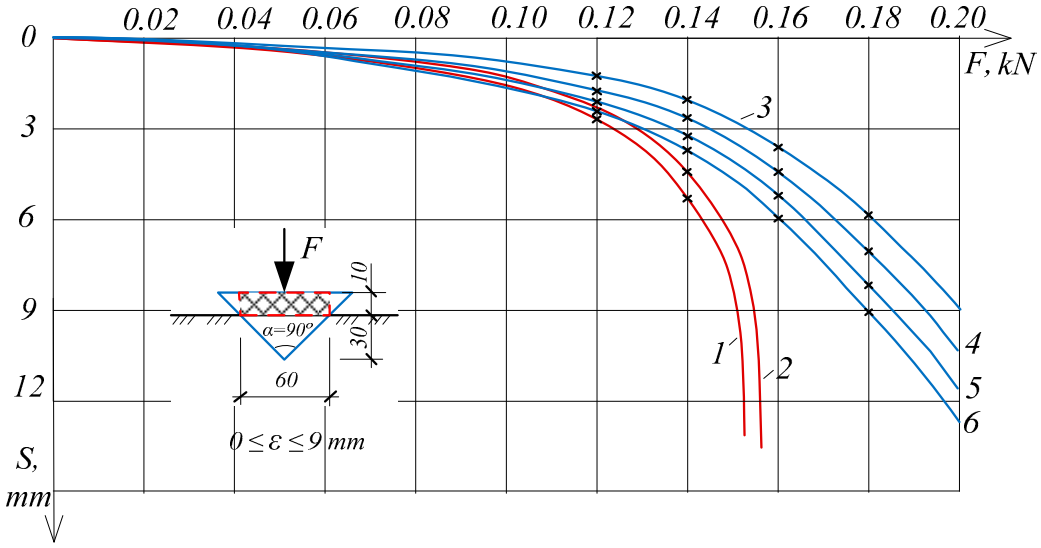

(**a**)

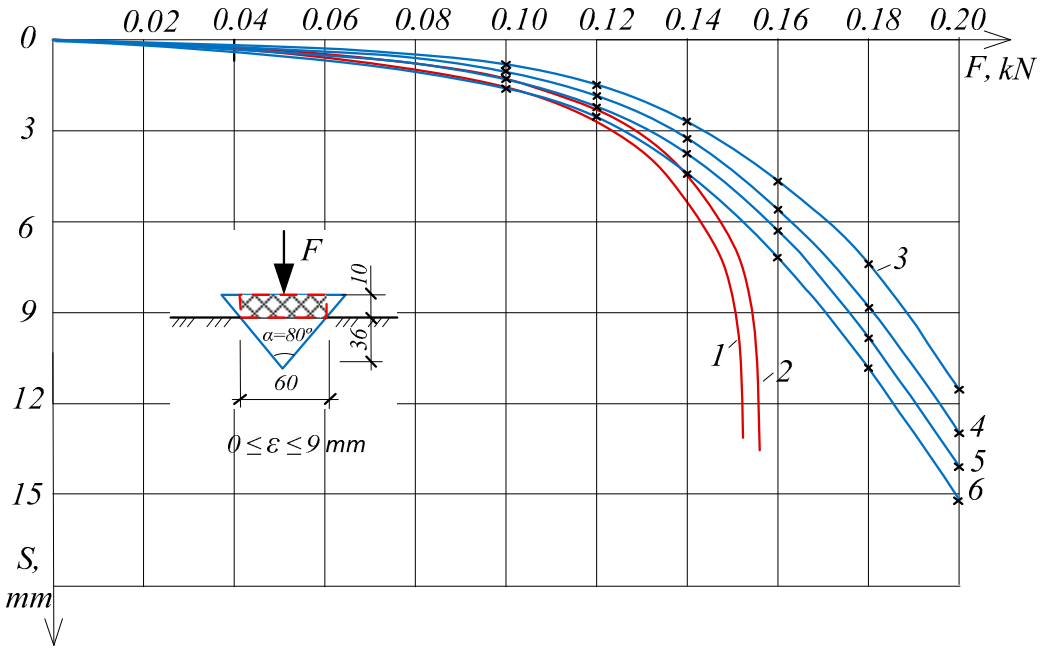

(**b**)

Figure 13. Results of laboratory studies on load–settlement monitoring: (**a**)—conical model with aperture angle 90°; (**b**)—conical model with aperture angle 80°; 1, 2—curves obtained for isolated shallow foundation for horizontal tensile strains ε = 0, 3 mm/m; 3, 4, 5, 6—curves obtained for conical foundation for horizontal tensile strains ε = 0, 3, 6 and 9 mm/m.

Table 4. Results of the laboratory modeling for loading–settlement interaction.

Foundation Model Type	Horizontal Tensile Strains of Soil, mm/m	Settlement under Load, mm					
		0.1 kN	0.12 kN	0.14 kN	0.16 N	0.18 kN	0.2 kN
Conical foundation with an aperture angle of 90°	0	0.77	1.21	2.03	3.60	5.82	8.96
	3	1.05	1.72	2.62	4.43	7.05	10.38
	6	1.35	2.10	3.23	5.12	8.02	11.51
	9	1.58	2.40	3.71	5.85	9.00	12.62
Conical foundation with an aperture angle of 80°	0	0.82	1.48	2.71	4.64	7.40	11.50
	3	1.05	1.82	3.28	5.62	8.72	12.91
	6	1.35	2.23	3.75	6.32	9.84	14.08
	9	1.61	2.58	4.42	7.21	10.53	15.15
Isolated shallow foundation	0	1.30	2.32	4.44	-	-	-
	3	1.53	2.71	5.25	-	-	-

Conical foundations with an aperture angle 90° showed superiority over the conical model of 80° aperture model and isolated shallow foundation. Settlement under a load of 0.2 kN without horizontal soil displacement reached 11 mm for conical foundations with an opening angle of 80° (Figure 13b), while for models with an aperture angle of 90° it did not exceed 9 mm. The presence of a horizontal displacement of up to 9 mm increased the soil settlement by 4 mm. Isolated shallow foundation models lost their bearing capacity after 0.14 kN.

The results of the laboratory testing for the loading–settlement interaction of conical and isolated shallow models of foundations are presented in Table 4.

Field test results were obtained for conical and isolated shallow foundations, observed before and after recorded horizontal movement at the experimental site of the Kostenko mine (Figure 14).

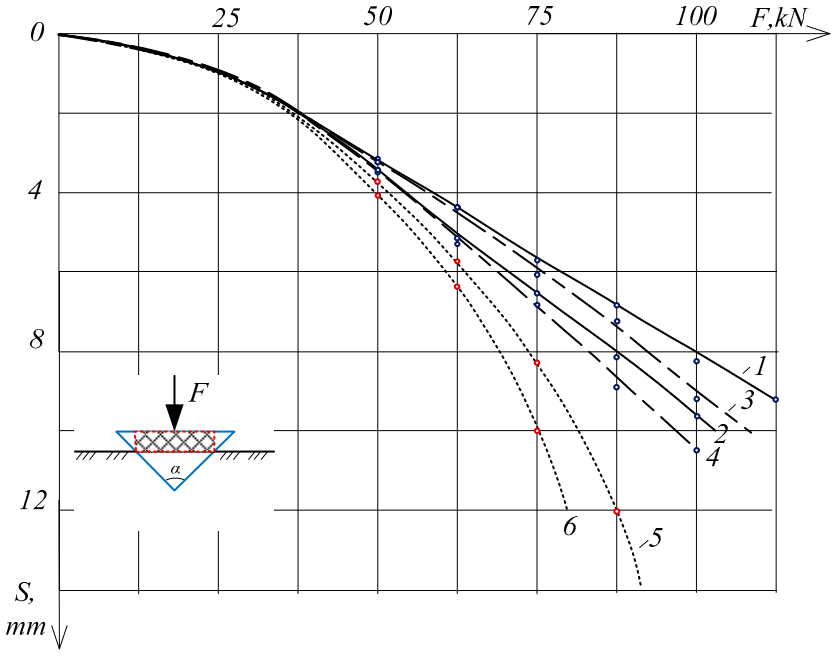

Figure 14. Results of full-scale loading tests: 1, 3—curves obtained for horizontal tensile strains ε = 0, conical foundations with an aperture angle of 90° and 80°; 2, 4—curves obtained for horizontal tensile strains ε = 2.6 mm/m, conical foundations with an aperture angle of 90° and 80°; 5, 6—curves obtained for horizontal tensile strains 0 and 2.6 mm/m for isolated shallow foundations.

The settlement under a load of 100 kN was 8.25 mm for conical foundations, with an aperture angle of 90° and 9.62 mm for foundations with an aperture angle of 80° (Table 5).

At the same time, a failure was observed for columnar foundations with a load of more than 80 kN. With horizontal tensile deformations $\varepsilon = 2.6 \times 10^{-3}$ m, the bearing capacity is reduced by 13–14% for conical foundations and by 8% for columnar-type foundation, although superiority in the load-bearing capacity of conical foundations is obvious already at a load of 50 kN. As the load rose, the increase in the cross-section of foundations was proportionally enhancing its load-bearing capacity.

Table 5. Field test results.

Foundation Model Type	Horizontal Tensile Strains of Soil, mm/m	Settlement under Load, mm		
		50 kN	75 kN	100 kN
Conical foundation with an aperture angle of 90°	0	3.21	5.72	8.25
	2.6	3.45	6.61	9.62
Conical foundation with an aperture angle of 80°	0	3.25	6.08	9.21
	2.6	3.50	6.85	10.50
Isolated shallow foundation	0	3.70	8.4	-
	2.6	4.10	10.0	-

The results of the numerical modeling are presented in Table 6. The total settlement for conical foundation with an aperture angle of 90° was 9.54 mm under a load of 0.2 kN at the first stage (without horizontal displacement of soils). Horizontal displacement of the soil by 3 mm led to a decrease in bearing capacity by approximately 0.008–0.010 kN for conical models of foundation. Each further displacement of the soil led to a decrease in bearing capacity by approximately 0.006–0.008 kN both for conical models with an aperture angle of 90° and 80°.

Table 6. Results of the numerical modeling for loading–settlement interaction.

Foundation Model Type	Horizontal Tensile Strains of Soil, mm/m	Settlement under Load, mm		
		0.1 kN	0.15 kN	0.2 kN
Conical foundation with an aperture angle of 90°	0	0.75	2.65	9.54
	3	1.02	3.30	11.24
	6	1.32	3.90	12.19
	9	1.55	4.50	13.51
Conical foundation with an aperture angle of 80°	0	0.80	3.40	11.51
	3	1.03	4.19	13.48
	6	1.30	4.80	15.50
	9	1.60	5.70	16.54
Isolated shallow foundation	0	1.30	7.25	-
	3	1.50	11.44	-

Numerical methods confirmed the stability of a conical foundation under horizontal soil displacements compared to isolated shallow foundations with the same cross-sectional area in contact with the ground surface. The discrepancies between settlements during laboratory tests and numerical modeling were no more than 9%.

4. Discussion

The presented study differs in the research method from [25–28], in that laboratory tests were performed on a three-dimensional expandable testing stand with simulating horizontal soil displacement. Moreover, conical foundations are proposed to be buried in the ground not to their full height, as in [25]. Solid conical foundation models were considered here, the operation of which differs from hollow cones in [23]. In this work, it also proposes a ball joint to eliminate horizontal forces in the upper part of the structure located above the base beam. Conical foundations were proposed to be used for the construction of buildings and structures in the form of a series of cones and not a single solid foundation to support a wind turbine, as was proposed by [24,25].

In the works of Li et al. [23], Nguyen Van et al. [24], Chouhan et al. [25], and Houlsby and Martin [26], conical foundations were designed with the base immersed to or below the ground level. In this work, considering the requirement of increased responsibility for civil engineering, installation depth of a conical foundation in the ground is recommended with partial immersion that provides a safety margin compared to an isolated shallow foundation. In this case, the load-bearing capacity increases in direct proportion to the insertion depth of conical block.

Experimental studies of the present research have demonstrated that in the elastic stage of deformation, the bearing capacity and settlement for conical and isolated shallow models are the same (Figure 15). With further loading of the foundation models, the penetration capacity of the conical shape of the foundation decreases due to an increase in the area of contact with the soil thickness. And for foundations with an isolated shallow cross-section, the support area is the same in height. For the same reason, according to the obtained load–settlement graphs, the maximum bearing capacity of conical foundations was not achieved.

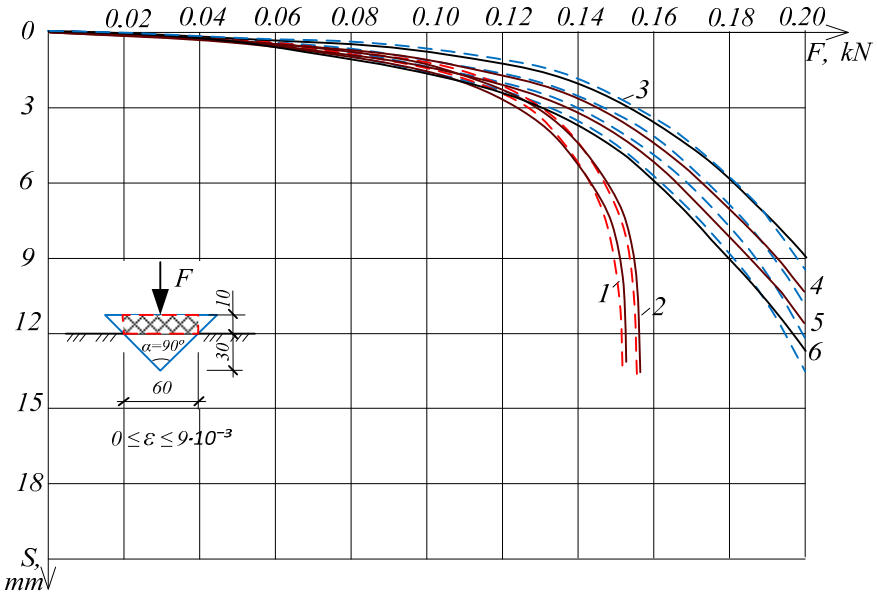

Figure 15. Comparison of results of numerical and laboratory methods for conical (with 90° aperture angle) and isolated shallow foundations: 1, 2—curves obtained for isolated shallow foundation with horizontal tensile strains ε = 0, 3 mm/m; 3, 4, 5, 6—curves obtained for conical foundation with horizontal tensile strains ε = 0, 3, 6 and 9 mm/m; ------numerical modeling results.

Laboratory tests are confirmed by the results of the numerical method with identical initial parameters of the soil and foundation models (Figure 15). Isolated shallow foundations lost their bearing capacity after 0.15 kN, while conical foundations continued to bear the load even under conditions of horizontal soil movement.

Field tests were limited to a horizontal soil movement of 2.6 mm, although they also confirmed the higher load-bearing capacity of conical foundations that are effective in areas of possible seismic activity and in mined areas. In this case, the horizontal forces caused by horizontal tensile strains of the soil mass can be eliminated by installing a special rolling joint located between the conical foundations and the plinth structure.

Analysis of the load–settlement graph in Figure 16 shows that the penetration of foundations with a conical base downwards into the soil increases as the horizontal tensile deformations increase. The dependence of settlement during undermining or tensile deformations in the soil according to [18,20] is equal to:

$$Su = S_0 \cdot (1 + D \cdot \varepsilon), \quad (7)$$

where D—is an empirical coefficient;

ε—horizontal tensile strains of the surface soils (tensile deformation), $0 \leq \varepsilon \leq 9 \times 10^{-3}$ m;

Su—settlement during undermining (with horizontal displacement of soils);

S_0—settlement without undermining (without horizontal displacement of soils).

Thus, to determine the expected settlement after horizontal tensile strains and soil displacement, the coefficient D was calculated equal to 56.5 for a conical foundation with an aperture angle of 90°, and 50 for conical foundations with an aperture angle of 80°. It should be noted that this parameter is determined for the equivalent soil used for the laboratory testing. For soils at the Kostenko mine (Kazakhstan), coefficient D was determined as 44.5 for conical foundations with an aperture angle of 90° and 39 for conical foundations with an aperture angle of 80°.

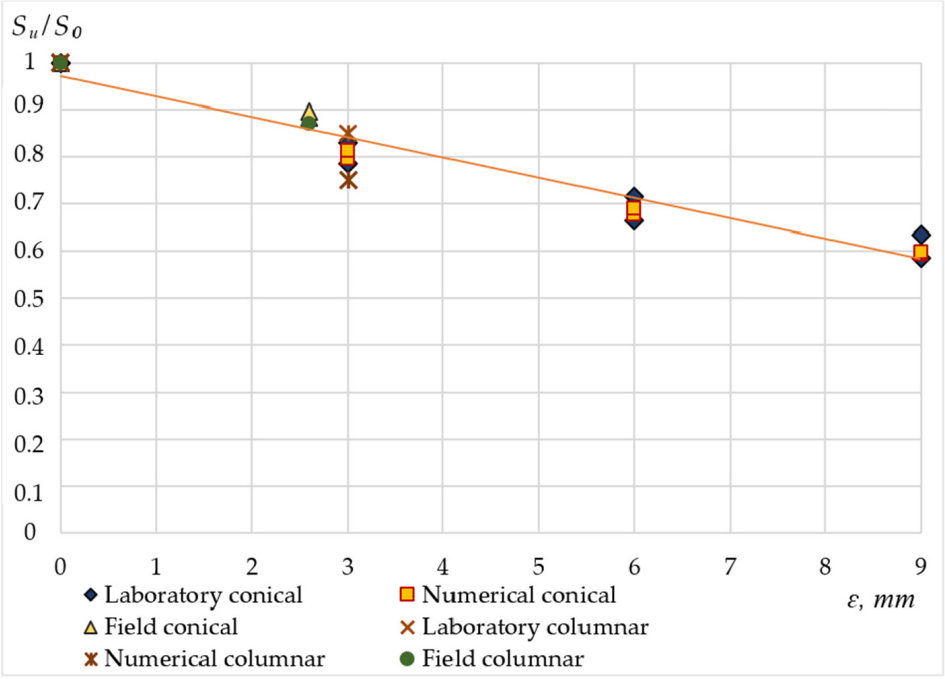

Figure 16. Graph of the relationship S_u/S_0 depending on tensile strains based on the results of numerical, field and model laboratory tests.

5. Conclusions

Based on the results of the study, the following points have been highlighted:

1. Laboratory, numerical and field testing confirmed the stability and higher load-bearing capacity of a conical foundation under horizontal tensile strains compared to isolated shallow foundations of the same cross-sectional area, at an intersection with the soil's surface.
2. The installation depth of a conical foundation in the ground with partial immersion provides advantages in the form of a safety margin compared to an isolated shallow foundation. In this case, the load-bearing capacity increases in direct proportion to the insertion depth of the conical block.
3. Model tests have shown that the bearing capacity of conical foundations enhance with the increasing angle of conus aperture and diameter of the foundation base. The discrepancies between calculations during laboratory tests and numerical modeling were no more than 9%.
4. Isolated shallow foundations lost their bearing capacity after 0.15 kN in laboratory tests and after 75 kN in the field tests, while the ultimate bearing capacity of conical foundations with a similar cross section at the soil surface was not achieved even

after 0.2 kN during laboratory tests with horizontal soil displacement and at a load of 100 kN in field tests.

5. The dependence of soil settlement after undermining and soil settlement before undermining on the magnitude of horizontal soil displacement for conical foundations was determined.

The horizontal tensile strains caused by the horizontal displacement of the soil mass in undermined or seismic areas can be eliminated by installing a special rolling joint located between the conical foundations and the plinth structure.

Author Contributions: Conceptualization, A.Z. and A.S.; methodology, A.Z. and B.B.; software, A.O.; validation, B.B., A.Z. and A.S.; formal analysis, A.S.; investigation, A.S. and B.B.; resources, A.Z.; data curation, A.S.; writing—original draft preparation, A.S.; writing—review and editing, A.S.; visualization, A.S.; supervision, A.Z.; project administration, A.S.; funding acquisition, A.S. All authors have read and agreed to the published version of the manuscript.

Funding: This work was funded by the Committee of Science of the Ministry of Science and Higher Education of the Republic of Kazakhstan, grant number AP13268861 «Development of structures of smart foundations in undermined and seismically hazardous territories».

Institutional Review Board Statement: Not applicable.

Informed Consent Statement: Not applicable.

Data Availability Statement: The raw data supporting the conclusions of this article will be made available by the authors on request.

Acknowledgments: The authors are grateful to the colleagues of Geotechnical Institute of the L.N. Gumilyov Eurasian National University and "KGS-Astana" for the provided administrative and technical support.

Conflicts of Interest: The authors declare no conflicts of interest.

References

1. Malinowska, A.; Hejmanowski, R. Building Damage Risk Assessment on Mining Terrains in Poland with GIS Application. *Int. J. Rock Mech. Min. Sci.* **2010**, *47*, 238–245. [CrossRef]
2. Bakhurin, I.M. *Movement of Rocks under the Influence of Mining*; State Scientific-Technical Publishing House of Petroleum and Mining Fuel Literature: Moscow, Russia, 1946; 231p.
3. Marschalko, M.; Fuka, M.; Treslin, L. Measurements by the Method of Precise Inclinometry on Locality Affected by Mining Activity. *Arch. Min. Sci.* **2008**, *53*, 397–414.
4. Marschalko, M.; Bednárik, M.; Yilmaz, I.; Bouchal, T.; Kubečka, K. Evaluation of Subsidence Due to Underground Coal Mining: An Example from the Czech Republic. *Bull. Eng. Geol. Environ.* **2012**, *71*, 105–111. [CrossRef]
5. Krutch, G. *Movement of Rocks and Protection of Undermined Structures*; Nedra: Moscow, Russia, 1978; 494p.
6. Pang, H.; Chen, C.; Xia, K.; Deng, Y.; Zhang, C.; Sun, C. A Methodology Based on Strain Analysis for Identifying Potential Discontinuous Deformation Zones in Sublevel Caving Mines. *Eng. Geol.* **2020**, *279*, 105872. [CrossRef]
7. Makarov, P.V.; Eremin, M.O. Rock mass as a nonlinear dynamic system. Mathematical modeling of stress-strain state evolution in the rock mass around a mine opening. *Phys. Mesomech.* **2018**, *21*, 293–296. [CrossRef]
8. Altun, A.O.; Yilmaz, I.; Yildirim, M. A Short Review on the Surficial Impacts of Underground Mining. *Sci. Res. Essays* **2010**, *5*, 3206–3212.
9. Muller, R.A. *The Influence of Mining Workings on the Deformation of the Earth's Surface*; Ugletekhizdat: Moscow, Russia, 1958.
10. Avershin, S.G. *Movement of Rocks during Underground Development*; Ugletekhizdat: Moscow, Russia, 1947.
11. Kozlov, V.P. *Research on the Interaction of Horizontal Foundation Deformations on the Foundations of Undermined Buildings and Structures*; Dissertation of a Candidate of Technical Sciences, Research Institute of Mining Geomechanics and Mine Surveying: Leningrad, Russia, 1979.
12. Marschalko, M.; Yilmaz, I.; Kubečka, K.; Bouchal, T.; Bednárik, M.; Drusa, M.; Bendová, M. Utilization of Ground Subsidence Caused by Underground Mining to Produce a Map of Possible Land-Use Areas for Urban Planning Purposes. *Arab. J. Geosci.* **2015**, *8*, 579–588. [CrossRef]
13. Yushin, A.I. *Features of Designing the Foundation of Buildings on Foundations Deformed by Mining Workings*; Yushin, A.I., Ed.; Stroyizdat: Moscow, Russia, 1980; 134p.
14. Baek, J.; Kim, S.-W.; Park, H.-J.; Jung, H.-S.; Kim, K.-D.; Kim, J.W. Analysis of Ground Subsidence in Coal Mining Area Using SAR Interferometry. *Geosci. J.* **2008**, *12*, 277–284. [CrossRef]

15. Usanov, S.V.; Konovalova, Y.P.; Usanova, A.V. Investigation of the Causes of Damage to Residential Low-Rise Buildings in the Zone of Influence of Underground Mining. *Proc. Tula States Univ. Sci. Earth* **2023**, *2*, 334–346. [CrossRef]
16. *SP RK 2.03-101-2012*; Buildings and Constructions in Earned Additionally Territories and Subsiding Soil. Committee for Construction, Housing and Communal Services and Land Management of the Ministry National Economy of the Republic of Kazakhstan: Astana, Kazakhstan, 2015.
17. *SN RK 2.03-01-2011*; Buildings on Undermined Territories and Soil Subsidence. Committee for Construction, Housing and Communal Services and Land Management of the Ministry national economy of the Republic of Kazakhstan: Astana, Kazakhstan, 2015.
18. Fadeev, A.B.; Kleshchev, P.E.; Zhussupbekov, A.Z. Variation in the Bearing Capacity and Pliability of Undermined Beds. *Soil Mech. Found Eng.* **1986**, *23*, 63–68. [CrossRef]
19. Zhussupbekov, A.Z.; Tanaka, T.; Aldungarova, A.K. The Effect of Reinforcement on Stability of Model of the Dam on Undermining Soil Ground. *JGS Spec. Publ.* **2016**, *2*, 1546–1550. [CrossRef]
20. Zhussupbekov, A.Z.; Frankovská, J.; Stacho, J.; Al-Mhaidib, A.I.; Doubrovsky, M.; Uranhayev, N.; Yerzhanov, S.; Morev, I. Geotechnical and Construction Considerations of Pile Foundations in Problematical Soils. *JGS Spec. Publ.* **2016**, *2*, 2704–2709. [CrossRef]
21. Lee, S.J.; Song, T.W.; Lee, Y.S.; Song, Y.H.; Kim, H.K. A case study of building damage risk assessment due to the multi-propped deep excavation in deep soft soil. In Proceedings of the 4th International Conference on Soft Soil Engineering, Vancouver, BC, Canada, 4–6 October 2006; Taylor Francis: London, UK, 2007.
22. Li, D.; Li, S.; Zhang, Y. Cone-Shaped Hollow Flexible Reinforced Concrete Foundation (CHFRF)—Innovative for Mountain Wind Turbines. *Soils Found.* **2019**, *59*, 1172–1181. [CrossRef]
23. Li, S.; Zhang, Y.; Li, D. Capacity of Cone-Shaped Hollow Flexible Reinforced Concrete Foundation (CHFRF) in Sand under Horizontal Loading. *Adv. Mater. Sci. Eng.* **2020**, *2020*, 6346590. [CrossRef]
24. Nguyen Van, C.; Keawsawasvong, S.; Nguyen, D.K.; Lai, V.Q. Machine Learning Regression Approach for Analysis of Bearing Capacity of Conical Foundations in Heterogenous and Anisotropic Clays. *Neural Comput. Appl.* **2023**, *35*, 3955–3976. [CrossRef]
25. Kritesh, C.; Qui, L.V.; Jitesh, C.; Kittiphan, Y.; Suraparb, K. Evaluation of vertical bearing capacity factors for conical footing with varying base roughness using FELA and MARS model. *Ships Offshore Struct.* **2023**, 1–13. [CrossRef]
26. Houlsby, G.T.; Martin, C.M. Undrained bearing capacity factors for conical footings on clay. *Géotechnique* **2003**, *5*, 513–520. [CrossRef]
27. Chakraborty, M.; Kumar, M. Bearing capacity factors for a conical footing using lower- and upper-bound finite elements limit analysis. *Can. Geotech. J.* **2015**, *52*, 2134–2140. [CrossRef]
28. Cassidy, M.J.; Houlsby, G.T. Vertical bearing capacity factors for conical footings on sand. *Géotechnique* **2002**, *52*, 687–692. [CrossRef]